

THE COMBUSTION RATES OF COAL CHAR: A REVIEW

I. W. SMITH

*CSIRO Division of Fossil Fuels
P.O. Box 136
North Ryde, NSW 2113, Australia*

A brief description is given of devolatilization of raw coal and combustion of the residual char. Major achievements in the study of devolatilization and important areas for further experimentation are noted; however, attention is focussed on the rate processes involved in char combustion.

Means of calculating reaction rates are shown which account for temperatures of particles, mass transfer and diffusion of oxygen into the particle's pore structure, and reaction on the pore walls. Theoretical consideration is then given to the changes in the size, density, and pore structure of chars as they burn.

Experimental data are shown for observed reactivities of coal chars corrected for external mass transfer effects, and intrinsic reactivities are reported for various coal chars and other carbons corrected for pore diffusion effects. Measured data on mass-transfer rates and changes in particle structure during combustion are given.

Recommendations are made for further research on char reactivity and the manner in which pore structure develops during combustion. The need for combustion-oriented kinetics studies of coal devolatilization is outlined.

Introduction

Solid fuels have a major and increasingly important role to play in combustion: pulverized fuel (pf) (coal ground to <0.2 mm in size) is used in many power generating plants whilst crushed coal (-10 mm in size) is used in small-scale appliances and fluidized-bed combustors. Advanced combustion processes, e.g. MHD power generation and coal injection as a supplementary fuel through the tuyères of blast furnaces, seek to burn pf at high intensities.

The need to burn increasing amounts of coal and related materials mainly arises from the need to replace oil and natural gas as fuels for combustion in furnaces. In addition to satisfying normal economic constraints, existing and new combustion processes must be able to burn low-grade fuels and satisfy local environmental requirements. Some requirements cause conflict, e.g. the combustion of low-grade fuels can be relatively costly due to reduced plant capacity and efficiency, and the costs incurred in controlling pollution levels.

In order to improve existing combustors and to develop new combustion techniques, it is necessary to gain an improved understanding of the complex processes that occur in and around particles during combustion. For example, better insights are needed into ignition stability, the attainment of rapid burn-out of particles, the nature of the various homo-

geneous and heterogeneous processes involved in generating gaseous pollutants and the routes by which inorganic constituents of fuels are converted into ash.

The combustion of most solid fuels involves two major steps: (i) the thermal decomposition (pyrolysis, devolatilization) that occurs during the initial heating, accompanied by drastic physical and chemical changes which usually involve the particle becoming plastic then rehardening, and (ii) the subsequent combustion of the porous solid residue (char) from the first step. The burning rate of the solid depends in part on the size of the char particle and the nature of its pore structure. These physical properties, together with important chemical properties, are affected by changes during the first step. The first step is rapid, the second is slow. In pf flames the time for devolatilization to take place is of the order of 0.1 s and for char burn-out the time is 1 s; for particles burning in fluidized-bed combustors the corresponding orders are 10 and 1000 s. Therefore the burning of the char has a major effect on the volume of the combustion chamber required to attain a given heat release.

In the following text a brief description is given of what is known, and what needs to be understood, about thermal decomposition. However the main aim of this review is to summarize the state of knowledge of the factors that govern the rate of

combustion of coal chars and related solids. The next section describes the behaviour of particles during combustion, including devolatilization. Subsequent sections deal with: Calculation of Particle Combustion Rates, Theoretical Relationships for Calculating Burning Rates, Experimental Data on Burning Rates, and Changes in Particle Structure During Combustion. In the Concluding Remarks emphasis is given to some key areas for further research.

Reliance is placed on earlier reviews to cover established ground: emphasis here is placed on new work and its consequences. The review deals mainly with the major solid fuel—coal. However the theory outlined below is applicable to the combustion of other solid fuels. Experimental data on mass transfer rates are applicable to any solid fuels.

Particle Combustion

Historical aspects of coal and carbon combustion have been outlined by Essenhig¹ and Mulcahy.² Field *et al.*³ and Smoot and Pratt⁴ have given comprehensive accounts of pulverized-coal combustion. Essenhig and his colleagues published a number of reviews on coal combustion⁵⁻⁹ and specific reviews on the mechanisms involved in coal-oxygen and related reactions have been given by Wendt,¹⁰ Mulcahy and Smith,¹¹ Hedley and Leesley,¹² and Laurendeau.¹³ Mulcahy² highlighted some of the more notable aspects of the carbon-oxygen reaction and Smith^{14,15} reviewed factors controlling the reactivity of pulverized-coal chars. The mechanisms of coal pyrolysis have been reviewed by Jüngten and van Heek,¹⁶ Anthony and Howard,¹⁷ and Howard.^{18,19} At the moment there is much interest in the mechanistic and technical aspects of coal pyrolysis as a step in the production of liquid fuels from coal,^{18,20} however, there is a notable lack of kinetic data relevant to combustion conditions.

The processes involved in the pyrolysis and combustion of particles are complex. Depending on the type of coal, the particle size, the relative rates of heating, decomposition, and oxygen transfer, volatile evolution and combustion of the solid may occur in separate stages or simultaneously.

Recent photographic studies of the behaviour of dilute suspensions of pulverized coals in the post-flame gases of small-scale gas burners^{21,22} showed that volatiles issue from bituminous coal particles (80 to 100 μm in size) in jets or trails, not always as spherically-uniform clouds (see Fig. 1). It is possible that, in regions of the particle surface where

there are no volatile jets, oxygen can attack the particle directly. No trails were shown for anthracites, lignites, or 40 μm particles of a bituminous coal.²² Particles (1 mm) of an Australian brown coal (lignite) showed heterogeneous combustion before the onset of volatile evolution.²³ Leslie *et al.*²⁴ working on the combustion of ~ 60 μm particles of Montana sub-bituminous coal at $\sim 7\%$ v/v oxygen, indicated that at gas temperatures about 1100 K particles burn by direct oxygen attack with little separate evolution of volatiles. However at 1600 K volatile evolution appears to precede the combustion of the solid particles.

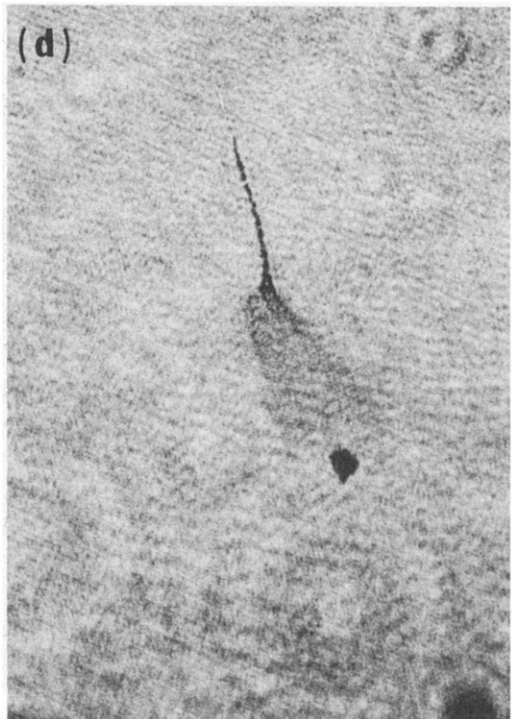
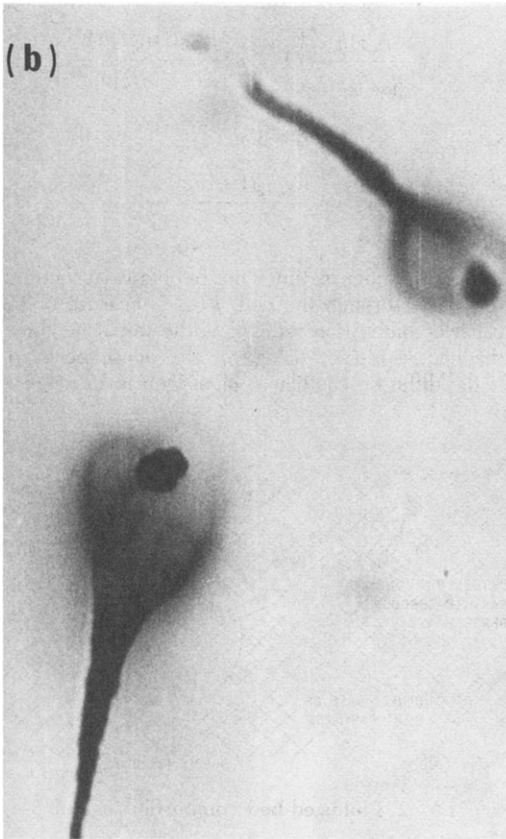
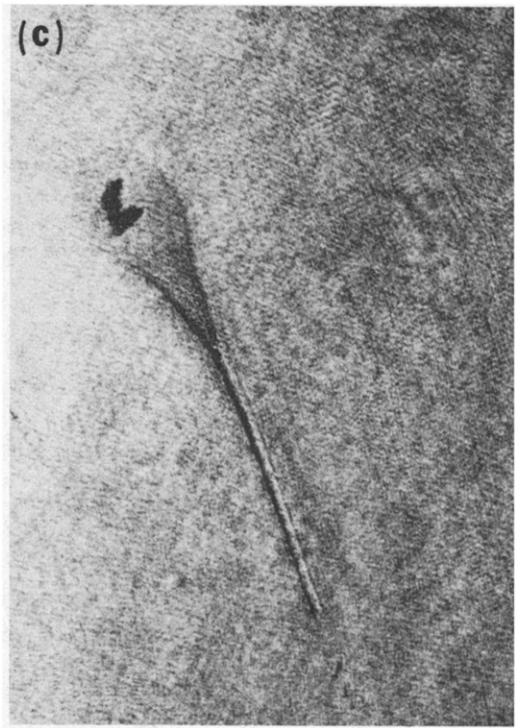
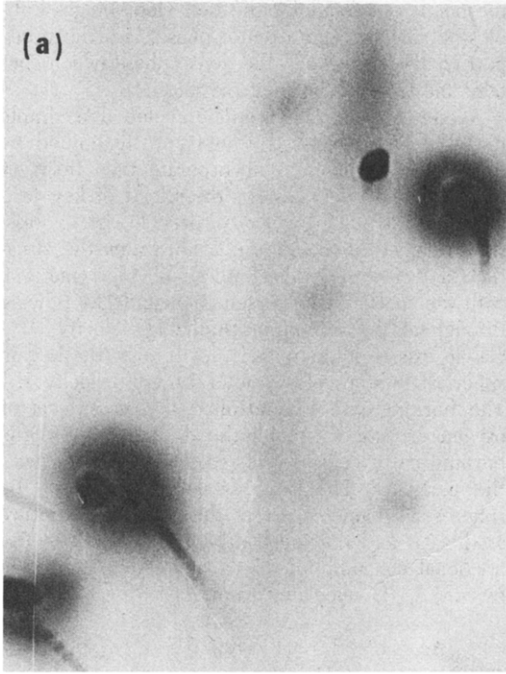
The behaviour of coals during pyrolysis depends on the factors already outlined, and on other conditions specific to particular combustors. In pf flames, coal is injected in a dense stream conveyed in a jet of air. Initial heating is mainly by hot gases recirculated into the jet. Particles in the centre of the jet are heated relatively slowly; those on the edge are heated rapidly and in the presence of high levels of oxygen. The amount of volatile matter produced, the nature of the pore structure, and the size of the resulting char particles depend on the rate of heating^{25,26} and on the level of oxygen.²⁷ During fluidized-bed combustion the injected fuel particles are heated rapidly, with much of the heating taking place by direct particle-to-particle contact. Tyler^{28,29} injected fine particles (~ 100 μm) of a wide range of coals into fluidized beds of sand. Over the temperature range 400 to 1000° C, in the absence of oxygen, coking and non-coking bituminous coals, sub-bituminous coals, and lignites all showed some degree of plastic behaviour and adhesion to other particles.

Useful studies have been made on the kinetics of pyrolysis of pulverized coal in entrainment,³⁰⁻³³ but little work has been done on coal behaviour under combustion conditions. Little attention has been given to the effects of the atmosphere (especially oxidizing) on pyrolysis, nor has there been adequate determination of the nature of the volatile products. Very few studies have been done on coal pyrolysis during fluidized-bed combustion. Some useful studies have been done³⁴⁻³⁶ but few data are available under the relevant chemical and physical conditions.

Calculations of Particle Combustion Rates

Usually calculations are made of the burning rates of a single particle or an assembly of particles, of the temperature of the particles by simul-

FIG. 1. Combustion of high-volatile bituminous coals: (a) Pittsburgh Seam, 65 μm , at ignition;²² (b) Pittsburgh Seam, 65 μm , after ignition;²² (c) Four Corners, 80 μm , ~ 10 ms reaction time;²¹ (d) Utah, 90 μm , ~ 5 ms reaction time.²¹



taneous heat balance, and of the effect the combustion process has on the surroundings, e.g. on the temperature and oxygen content of the ambient gas.

There are many mathematical models of various types of particle combustion systems.^{3a,37-39} Based on Field *et al.*,^{3a} McKenzie *et al.*^{40,41} modelled the combustion of a polydisperse suspension of pf particles in plug flow. Their treatment showed fractional burn-off (extent of combustion), u , to be related to time, t , by:

$$\frac{du}{dt} = \frac{6}{d_o \sigma_o} y^{1-\alpha-\beta} \rho \quad 1/s \quad (1)$$

where $y = 1 - u$, α and β are coefficients in the expressions relating respectively the changes in particle size (d) and density (σ) to burnoff (see Eqs. (27) and (28)), subscript o refers to initial conditions ($u = 0$) and ρ is the actual (observed) rate of combustion of carbon per unit external surface area of the particle.

The change of particle temperature, T_p , with time is given by:

$$\frac{dT_p}{dt} = \frac{12}{C_p} \left[\frac{du}{dt} \frac{H}{y} - \phi_1(T_p - T_g) - \phi_2(T_p^4 - T_s^4) \right] \quad K/s \quad (2)$$

where C_p is the specific heat of the particle, T_g and T_s are the temperatures of the surrounding gas and radiating surfaces respectively, ϕ_1 and ϕ_2 involve convective and radiative heat transfer coefficients respectively and depend on particle size and density. H is the heat of reaction which depends strongly on the nature of the combustion process. At flame temperatures carbon burns to produce carbon monoxide, i.e. $C + 1/2 O_2 \rightarrow CO$ in which case $H \sim 2300$ cal/g. However, if the carbon monoxide oxidizes with sufficient speed to be completely burned before leaving the particle the heat of reaction is that appropriate to the step $C + O_2 \rightarrow CO_2$, i.e. $H \sim 7900$ cal/g.

Equations (1) and (2) can be used to calculate the behaviour of polydisperse suspensions when the equations are evaluated simultaneously for each size fraction, as well as using other relationships to calculate the corresponding changes in the properties of the ambient gas. The equations can also be used to calculate the behaviour of monodisperse suspensions, or the behaviour of a single particle.

The situation in fluidized-bed combustors, and consequently the equations for calculating combustion behaviour, are more complex⁴²⁻⁴⁴ than for plug-flow entrainment systems. This is because of

the need to account for the behaviour of gas bubbles passing through a dense phase, and the transport of oxygen through the dense phase which contains most of the burning particles.

Avedesian and Davidson⁴⁵ developed a simple model for fluidized-bed combustors, extended by Leung and Smith⁴⁶ to incorporate the effects of fuel reactivity, which allows the effects of key variables, e.g. fluidizing velocity, particle size, bubble size, to be studied. Figure 2 illustrates the situation: a well-mixed dense phase of inert material with fuel particles dispersed in it and gas flowing through at the minimum fluidizing velocity, U_m . Gas in excess of this passes up through the bed in spherical bubbles of diameter, d_b , at velocity U_b . The burning rate is controlled by the effects of oxygen exchange through the dense phase to the burning particles, and the reaction of oxygen with the particles. The particles are assumed to be spheres of diameter, d , at the same temperature as the gas and the inert material of the bed. The fractional consumption of oxygen fed to the combustor, A_o , is calculated from:

$$A_o = 1 - \gamma_o - (1 - \gamma_o)^2 / (k' - 1 - \gamma_o) \quad (3)$$

$$\text{where } \gamma_o = [(Z - 1)/Z] \exp(-X) \quad (4)$$

$$X = \frac{6.34h_o}{d_b(d_b/g)^{0.5}} \left[U_m + \frac{1.3\epsilon(DP_o/P)^{0.5}}{(1 + \epsilon)(d_b/g)^{0.25}} \right] \quad (5)$$

$$Z = U_b/U_m \quad (6)$$

$$k' = \frac{6V_e h_o (1 - \epsilon)}{d U_m Z} \cdot \frac{\rho}{C'_g} \quad (7)$$

X is the number of times the bubble is flushed out as it rises through the bed, k' is a measure of the particle combustion rate, h_o is the initial height of the bed, ϵ is the voidage of the dense phase, D is the diffusion coefficient of oxygen in nitrogen at

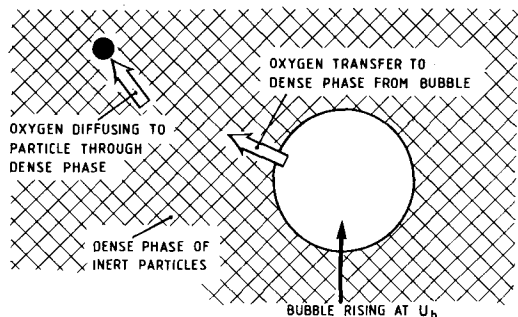


FIG. 2. Fluidized-bed combustion model.

combustion temperature and reference pressure P_0 , and P is the combustion pressure. V_c is the volume fraction of carbon and C'_g is the oxygen concentration in the dense phase.

For the calculations it is necessary to know, amongst other things, the value of ρ and its response to temperature and oxygen concentration, the manner by which particle size and density change during combustion, and the appropriate value for the heat of reaction, H .

Theoretical Relationships for Calculating Burning Rates

Observed Kinetics

Figure 3 illustrates the circumstances close to a burning particle. From mass-balance considerations the burning rate, ρ , can be expressed as:

$$\rho = h_m(C_g - C_s) = R_c(C_s)^n \quad \text{g/cm}^2\text{s} \quad (8)$$

where C_s is the oxygen concentration at the outer surface of the particle, C_g is the oxygen concentration in the bulk gas, R_c is a chemical rate coefficient of apparent order n in C_s , and h_m is the mass transfer coefficient discussed below.

Manipulation of Eq. (8) to eliminate the generally unknown C_s , gives a relationship for calculating ρ :

$$\rho = C_g^n(1 - \chi)^n R_c \quad \text{g/cm}^2\text{s} \quad (9)$$

where $\chi = \rho/\rho_m$ (10)

ρ_m is the product $h_m C_g$, the maximum possible

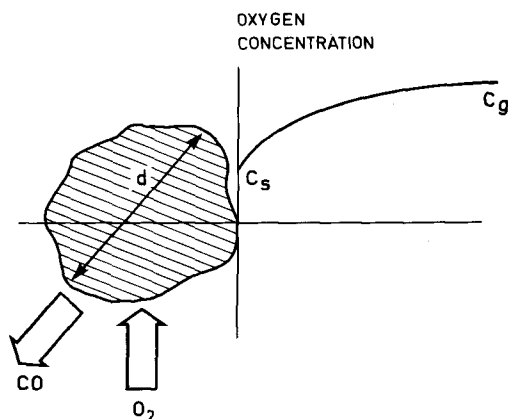


FIG. 3. Diagrammatic representation of a carbon particle burning in oxygen.

combustion rate, found when chemical reactions are so fast that $C_s \rightarrow 0$, and the burning rate is controlled solely by mass transfer of oxygen to the particle. Note that χ can never be greater than 1.

A further useful equation involving χ , derived analytically,⁴⁷ is:

$$\chi/(1 - \chi)^n = R_c C_g^n / \rho_m = R_c C_g^{n-1} / h_m \quad (11)$$

Equation (11) shows that χ depends on the order n . Because χ can be determined experimentally without any knowledge of n , Eq. (11) can be used in the determination of n .⁴⁷⁻⁴⁹

Equation (8) can be manipulated to give relationships for specific values of n . For $n = 1$ the familiar result is:

$$\rho = C_g/(1/h_m + 1/R_c) \quad \text{g/cm}^2\text{s} \quad (12)$$

For $n = 0^6$:

$$(\rho - \rho_m)(\rho - R_c) = 0 \quad \text{g}^2/\text{cm}^4\text{s}^2 \quad (13)$$

which shows that for zero order reactions that $\rho = R_c$ when there is a finite concentration of oxygen at the particle's surface ($C_s > 0$), and that the rate changes abruptly to give $\rho = \rho_m$ when $C_s = 0$.

Particle Reactivity

The coefficient R_c is referred to above as a "chemical" rate coefficient, but its response to temperature and oxygen concentration, its dependence on particle size and its variation during the combustion of the particle, are the results of three interacting factors: (i) the intrinsic rate of chemical reaction of oxygen with the internal surface of the particle, (ii) the extent of this surface, and (iii) the extent to which oxygen diffusion through the pores (which form the internal surface) restricts the reaction rate. The relationship between ρ (and hence R_c) and the coefficient of intrinsic chemical reactivity, R_i (the rate of reaction per unit area of pore wall per [unit concentration of oxygen] ^{m} in the absence of any mass transfer or pore diffusional limitation) is given by:

$$\rho = \eta \gamma \sigma A_g R_i [C_g(1 - \chi)]^m \quad \text{g/cm}^2\text{s} \quad (14)$$

where γ is the characteristic size of the particle (ratio of the volume to external surface area⁵⁰), A_g is the particle's specific area, m is the true order of reaction in the concentration of oxygen and η is the effectiveness factor, the ratio of the actual combustion rate to the rate attainable (all else being equal) if no pore-diffusion resistance existed. η is

a function of the Thiele modulus,⁵¹ ϕ , and can be calculated from:*

$$[\eta\phi^2(m+1)/2] \\ = \gamma\rho(m+1)/[8D_eC_g(1-\chi)] \quad (15)$$

where D_e is the effective coefficient for diffusion through the pore structure, calculated as shown below. The terms on the right hand side of Eq. (15) can all be measured, thus allowing $\eta\phi^2(m+1)/2$ to be calculated from experimental data. Then η (and hence R_i by Eq. (14)) can be determined using the relations between η and $\eta\phi^2(m+1)/2$ given by Mehta and Aris.⁵²

When chemical reactions are sufficiently slow, pore diffusion has no rate-limiting effect, the oxygen concentration throughout the pore is C_s and $\eta = 1$. Equation (14) then becomes:

$$\rho = \gamma\sigma A_g R_i [C_g(1-\chi)]^m \quad \text{g/cm}^2\text{s} \quad (16)$$

For these circumstances (kinetic regime I^{53,54}) ρ varies with particle size, and shows the true order of reaction, m , and the true activation energy when R_i is expressed in Arrhenius form. During combustion the particle density decreases but the size remains constant. When pore diffusion as well as chemical reaction has a strong rate-limiting effect⁵² (kinetic regime II,^{53,54}) the term $\eta\phi^2(m+1)/2 \rightarrow 1/\eta$,⁵² then Eqs. (14) and (15) give:

$$\rho = 2 \{2 A_g \sigma D_e R_i [C_g(1-\chi)]^{m+1}/(m+1)\}^{0.5} \\ \text{g/cm}^2\text{s} \quad (17)$$

Equation (17) is the familiar relationship derived, for example, by Frank-Kamenetskii⁵⁵ specifically for regime II conditions. In these circumstances ρ is independent of particle size, shows an apparent order, n , given by:

$$n = (m+1)/2 \quad (18)$$

and has an apparent activation energy about half that found for R_i . As combustion proceeds, large particles shrink as they burn at constant density.

*Jamaluddin *et al.*¹²⁰ recently pointed out that the equations used earlier to calculate R_i ⁵⁹ incorrectly used $\gamma/2$ rather than γ as the characteristic size. Hence Eqs. (15) and (17) are incorrect and there are errors in the reported values of R_i ⁵⁹ of up to a factor of 4 when pore diffusion has a strong effect. The error does not significantly change the kinetic conclusions of reference 59. However, if use is made of the reported values of R_i to calculate R_c or ρ the correct result will be gained using $\gamma/2$ rather than γ .

For pf-size particles, where the depth of penetration of oxygen into the pores is of the order of particle size,¹¹ both density and size of the particles reduce with burn-off.

Numerical values of R_c and R_i , and functions of these terms, are given for various carbons in the section on Experimental Data on Burning Rates. The data are shown in Arrhenius form:

$$R_c(\text{or } R_i) = A \exp[-E/(RT)]^\kappa \\ \text{g/cm}^2\text{s(atm)}^\kappa \quad (19)$$

where A is the frequency factor, E is the apparent or true activation energy as appropriate and κ is the corresponding apparent or true order. For convenience, rates are related to the partial pressure of oxygen.

Effective Pore Diffusion Coefficient, D_e , and Models of Pore Structure

The effective pore diffusion coefficient, D_e , is related to unit cross-sectional area of porous material and thus incorporates the effect of the number and size of the pores in the unit cross-section and the tortuosity (τ) of these pores. Satterfield⁵⁶ gives a useful review of theoretical and measured values of D_e . From the simple pore-structure model of Wheeler,⁵⁷ D_e can be calculated by:

$$D_e = D_p\theta/\tau \quad \text{cm}^2/\text{s} \quad (20)$$

where θ is the porosity of the solid and D_p is the diffusion coefficient through the pore. For large pores ($>1 \mu\text{m}$ in size when bulk diffusion occurs), D_p is equal to the molecular diffusion coefficient. For pores $<1 \mu\text{m}$ in size Knudsen diffusion occurs and D_p is given by:

$$D_p = 9.7 \times 10^3 \bar{r}_p (T_p/M)^{0.5} \quad \text{cm}^2/\text{s} \quad (21)$$

where M is the molecular weight of the diffusing gas and \bar{r}_p is the mean pore radius calculated by⁵⁷

$$\bar{r}_p = 2\theta\tau^{0.5}/A_g\sigma \quad \text{cm} \quad (22)$$

For most coal chars the majority of the surface area is associated with pores well below $1 \mu\text{m}$ in size, therefore Knudsen rather than bulk diffusion is more important for these materials.

There are two points that need to be made concerning the relation between pore diffusion and structure. Firstly the model used so far is a very simple representation of a rather complex physical situation.⁵⁷⁻⁵⁹ The tortuosity factor, τ , is used to correct calculated values of D_e to the extent that

they differ from measured values—factors of more than 10 are not unknown.⁵⁶ Indeed these factors are mainly for the correction of simplified models of pore structure and diffusion processes. Wheeler's model, giving rise to Eqs. (20) to (22), assumes that the pores can be adequately represented as a mono-disperse system. It is well known, however, that chars have a wide distribution of pore sizes, and that the size distributions are often polymodal. Smith and Tyler⁵⁸ developed a restricted model for reaction in semi-anthracite particles with a polymodal distribution of pore sizes. They found the intrinsic reactivity was essentially the same calculated by their bimodal and unimodal models. Other models are available for reactions in bimodal systems of porous solids⁶⁰⁻⁶² and for solids with Gaussian and Maxwellian distributions of pore sizes.⁶³

The second point on pore diffusion and structure concerns the non-steady state of the situation. Due to reaction, pores open up, changing in size and shape. Pore surface areas increase and may ultimately decrease due to coalescence. Therefore under regime I conditions rates vary with the fractional degree of burn-off, increasing as pore area increases and ultimately decreasing as pores coalesce or as expanding macropores "engulf" micropores. It is difficult, however, to make a generally useful model for such a situation. Some carbons (though not many) show rates that increase steadily with burn-off, other decrease steadily.⁶⁴ Nonetheless there have been a number of attempts to model evolving pore structures. Simons and co-workers,⁶⁵⁻⁶⁸ extending the treatment by Chornet *et al.*,⁶⁹ modelled the "engulfing macropore" system. Bhatia and Perlmutter⁷⁰ developed a random-pore model for fluid-solid reactions, and Srinivas and Amundson⁷¹ modelled the gasification of char accounting for progressive pore growth. Gavalas^{72,73} set up a model of spatially-random cylindrical pores. Simons⁷⁴ and Gavalas⁷⁵ compared some of the merits of their respective models.

Under regime II conditions an increase in pore size leads to an increase in pore diffusion rates and changes in the amount of pore surface available for reaction. There have been few attempts to develop theoretical models for such circumstances. Petersen⁷⁶ treated reactions in a single pore and in an array of pores which were initially uniform in size; Hashimoto and Silveston^{63,77} related changes in the effectiveness factor, η , with burn-off during gasification of carbon with a polydisperse pore system; Ramachandran and Smith⁷⁸ examined the effect on diffusion when a pore changed size due to the deposition or removal of solid. Gavalas⁷³ developed his earlier model⁷² to allow for the effect of pore diffusion, as well as external mass transfer, during the combustion of char particles. Kriegbaum and Laurendeau⁷⁹ modelled the gasification of char containing conical pores, having a polymodal distribu-

tion of sizes. Smith and Tyler⁵⁸ showed that where it is appropriate to treat the pores as mono-sized and where Knudsen diffusion is occurring, the observed rate in regime II can be calculated from a knowledge of the intrinsic reactivity and the porosity of the carbon alone. Holve⁸⁰ extended the treatment by Smith and Tyler to account for changes in porosity during combustion. Srinivas and Amundson⁸¹ dealt with the effects of pore diffusion in evolving bimodal pore structures.

Mass Transfer Coefficient, h_m

In practical combustion systems the transfer of oxygen to the burning particle often contributes notably to rate limitation. Indeed in the case of fluidized-bed combustion little, if any, limitation is imposed by chemical rates.^{45,46} Therefore in order to calculate ρ it is usually necessary to know the mass transfer coefficient, h_m .

For gas-solid systems, in fixed or fluidized beds or in entrainment, the relationship between h_m and the nature and state of flow of the ambient gas is given by equations of the form:^{36,82,83}

$$Sh = h'_m d/D = 2(1 + B Re^{1/2} Sc^{1/3}) \quad (23)$$

where Sh , Re , and Sc are the Sherwood, Reynolds', and Schmidt numbers respectively, B is a constant and h'_m is the mass transfer coefficient with respect to the flux of oxygen. To calculate Re , and hence h'_m , a knowledge of the gas velocity past the particle is required. In fluidized beds this is difficult to define. La Nauze and Jung,⁸⁴ for example, used the superficial gas velocity through the combustion vessel, modified to take account of the average voidage of the bed (see below).

In pf combustion, relative velocities between gas and particle are usually sufficiently small that Re can be set equal to zero.^{3c,11} There is little error if the particles are treated as spheres.^{3d} Then $Sh = 2$, the result obtained analytically for a sphere in a stationary gas, whence:

$$h_m = 0.75 D_o(P_o/P)(T_m/T_o)^{1.75}/d \quad \text{cm/s} \quad (24)$$

where T_m is the mean temperature of the boundary layer around the particle and subscript o denotes reference conditions. The factor 0.75 is the conversion involved in changing from h'_m (for oxygen flux) to h_m (for carbon oxide flux) and assumes the primary product of reaction to be CO , i.e. combustion is by $C + 1/2 O_2 \rightarrow CO$, as noted above.

In the case of fluidized-bed combustion the appropriate value of h_m for the flux of gases through the dense phase of inert particles around the burning particle is less well defined.^{83,85-88} Recent work⁸⁴ suggests a modification of Eq. (23) to account for the voidage, ϵ , of the dense phase:

$$\text{Sh} = 2\epsilon + 2B(\text{Re}/\epsilon)^{1/2}\text{Sc}^{1/3} \quad (25)$$

The suitability of Eq. (25) is discussed in the sections on experimental values of the mass transfer coefficient.

Changes in Particle Size and Density

The weight (W) of a particle is related to its initial weight (W_0) and the fractional degree of burn-off (u) by:

$$W = W_0(1 - u) \quad \text{g} \quad (26)$$

whence (for spheres or cubes):

$$d = d_0(1 - u)^\alpha \quad \text{cm} \quad (27)$$

$$\text{and} \quad \sigma = \sigma_0(1 - u)^\beta \quad \text{g/cm}^3 \quad (28)$$

where $3\alpha + \beta = 1$. For particles that burn with steadily reducing size and constant density $\alpha = 1/3$ and $\beta = 0$. However if size remains constant whilst density decreases $\alpha = 0$ and $\beta = 1$.

Equations (27) and (28) apply for particles with a homogeneous structure of pores that are small compared with particle size. In fact whilst coal chars are porous they do not have a simple pore structure: chars often contain large internal voids (of dimensions of the order of particle size) surrounded by microporous material⁸⁹⁻⁹¹. In pf flames, bituminous coals often form thin-walled cenospheres.⁹² In these circumstances a better, though still approximate, model is that of a hollow sphere with a wall of homogeneously-microporous material.⁸⁹ For complete penetration of oxygen into such a particle $\alpha = 0$ and $\beta = 1$, i.e. the particle would burn with a steady reduction in density but at constant size. For reaction confined to the outer surface of such a particle it can be shown that:

$$d = d_0(1 - u + ux^3)^{1/3} \quad \text{cm} \quad (29)$$

and

$$\sigma = \sigma_0(1 - u)/(1 - u + ux^3) \quad \text{g/cm}^3 \quad (30)$$

where x is the radius of the inside to the initial outside diameter of the particle. For the case of no internal voids, $x = 0$, then with $\alpha = 1/3$ and $\beta = 0$, Eqs. (29) and (30) reduce to Eqs. (27) and (28) respectively. At the other extreme, as $x \rightarrow 1$, i.e. for a thin-walled cenosphere, Eqs. (29) and (30) show that the particles burn at constant size and with steadily reducing density, even if reactions are confined to the outer surface.

Experimental Data on Burning Rates

Rate Coefficient, R_c

In order to determine R_c , it is necessary to carry out experiments that satisfy a number of conditions: measurements must be made with single particles or closely-sized materials⁹³ in order to relate rates to particle size, to correct for external mass transfer effects (i.e. correct for the extent that C_s differs from C_g) and to allow the determination of the changes in particle size and density with burn-off. The effects of changes in oxygen concentration and particle temperature need to be determined separately. Because of the need to know the initial properties of the material studied and because major changes occur in coal structure (chemical and physical) during devolatilization, it is necessary to use chars prepared separately under conditions found in the initial stage of the relevant coal combustion system.

Few experimental studies satisfy the above criteria. The data given here arise mainly from two suitable series of experiments. One series, due to Field and co-workers^{91,94,95} of the British Coal Utilization Research Association was performed using direct measurement of the weight loss of particles carried in laminar flow through a reactor for a known reaction time. The second series was carried out by CSIRO workers,⁹⁶⁻⁹⁸ who measured the progressive burn-away of particles in a plug-flow reactor using gas analysis techniques.

The purpose here is to report and compare values of reactivity for various chars. However a difficulty arises because not all chars show the same dependence of reactivity on oxygen concentration, i.e. n can change from char to char. In order to compare reactivities on a common basis the data are given, where necessary, in the form of a rate, ρ_c , defined by:

$$\rho_c = R_c(p_{\text{O}_2})^n \quad \text{g/cm}^2\text{s} \quad (31)$$

Firstly values of R_c are considered for petroleum coke. Figure 4 shows the relation between R_c and T_p in Arrhenius form for four sized fractions of coke, of median sizes 18, 77, 85, and 88 μm .^{98,49} It has previously been shown^{11,95-98} that the independence of R_c on particle size, and the apparent activation energy of ~ 20 kcal/mol (about half the value shown by impure carbons burning under regime I conditions⁵⁹) are consistent with reaction under regime II conditions. What has been less clear is the appropriate value of the observed reaction order, n .

Smith⁹⁸ reported rate data for petroleum coke burning at oxygen partial pressures close to 0.2 atm, assuming $n = 1$. Young^{49,99} burned petroleum

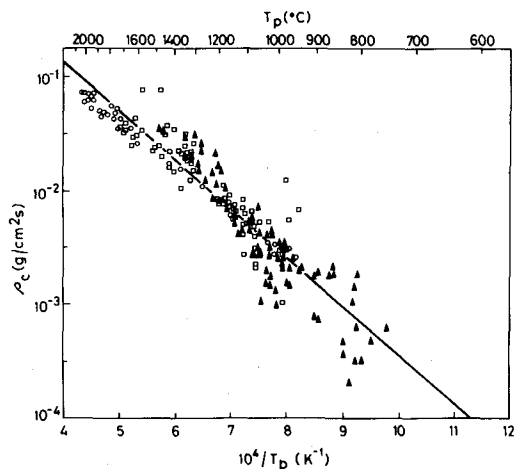


FIG. 4. Effect of temperature on ρ_c for petroleum coke (\square 18 μm ,⁹⁶ \circ 77 μm ,⁹⁶ \blacktriangle 85 and 88 μm ⁴⁹).

coke at oxygen pressures over the range 0.05 to 0.3 atm and used statistical techniques to analyse his results. He found least scatter in Arrhenius plots of data (the sum of the squares of the residuals at a minimum) at n close to 0.5 (see Fig. 5). From the evidence already noted the reaction is probably under regime II conditions, when Eq. (18) shows that the true order, m , is close to zero. Young¹⁰⁰

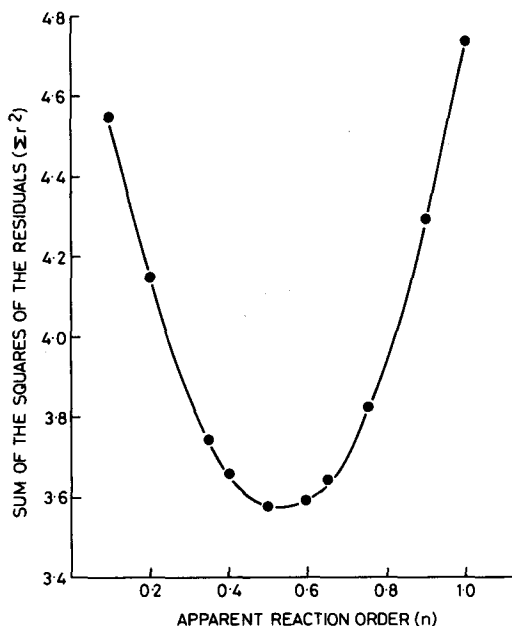


FIG. 5. Sum of the square of the residuals versus the apparent reaction order.

also found a value of $n \approx 0.5$ for a char produced by the flash pyrolysis of an Australian bituminous coal.¹⁰¹ Likewise a value of $n \approx 0.5$ was determined by Hamor and co-workers^{47,48} for an Australian brown coal char.

It is known that the true order of reaction depends on temperature and on the concentration of oxygen.^{11,102} It is more than likely, all else being equal, that the order will also depend on the nature of the carbon being oxidized.⁹⁹ There are practical difficulties in determining the true order in the presence of pore diffusion limitations—a change in the true order from zero to unity would only result in an apparent change from 0.5 to 1 (Eq. (1)). Few experiments have used a sufficiently wide range of oxygen concentrations for adequate determination of m . This is illustrated by the careful experiments of Field⁹¹ on the combustion of sized fractions of pf char (median sizes 28, 38, 82, and 105 μm) at 0.05 and 0.1 atm oxygen. Field's data have been reanalysed⁴⁹ and are shown in Arrhenius form in Fig. 6. The upper part of the diagram shows results from $n = 1$, the lower for $n = 0.5$. Application of the statistical analysis referred to above shows no significant difference using either of the orders. Field's results show an activation energy of ~ 20 kcal/mol, and an independence of R_c on particle size, i.e. his char was probably burning under regime II conditions.

Encouraging agreement is found in values of R_c determined for similar materials by workers using various techniques. Figure 7 shows results for anthracites and semi-anthracites determined on sized fractions of materials by Field,⁹⁵ Field and Roberts,⁹⁴ and Smith,⁹⁷ together with results for flames of polydisperse materials (Marsden,¹⁰³ Hein,¹⁰⁴ Beér *et al.*¹⁰⁵). With the exception of the pioneering work of Beér, the results are all within a factor of 2 above or below the median level. The data in Fig. 7 for sized materials show R_c to be independent of particle size; this fact together with the apparent activation energy of about 20 kcal/mol, supported by the observed changes in particle size and density during combustion,^{95,97} shows the reaction to be under regime II conditions. Similar conclusions were made for the combustion of 89 and 49 μm fractions of a brown coal char.^{47,48} However 22 μm particles of this char showed lower values of R_c (and possibly a higher value of activation energy) than the larger particles. Likewise values of R_c for 4 μm petroleum coke particles⁹⁸ and 6 μm semi-anthracite particles⁹⁷ were found to be lower than the corresponding values for larger particles. The fine particles were shown by measurement, calculation, or both, to be reacting under regime I conditions, or in the transition between regimes I and II.

Figure 8¹⁰⁶ shows the relationship between ρ_c

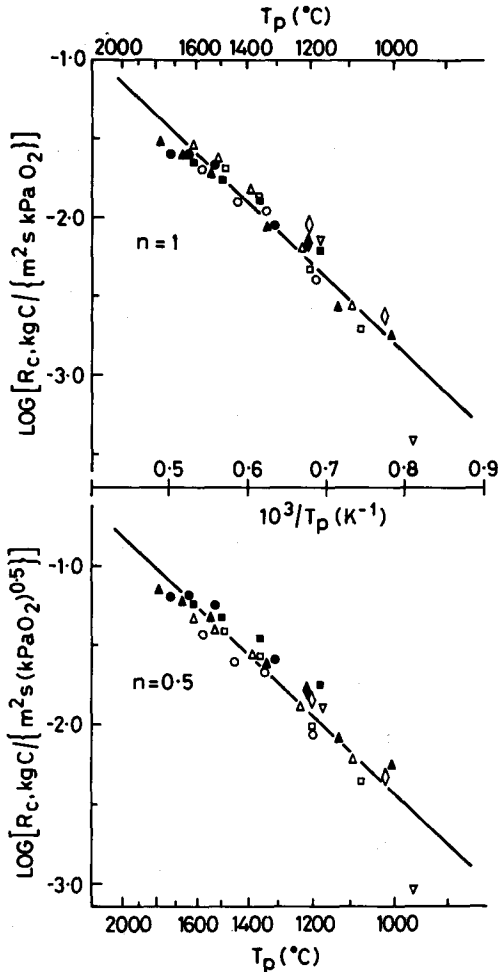


FIG. 6. Arrhenius diagram relating R_c to temperature replotted from Field's data⁸⁹ for a low rank char. Initial particle size: 28 μm (\square , \blacksquare), 28 μm (\circ , \bullet), 38 μm (\triangle , \blacktriangle), 82 μm (∇), 105 μm (\diamond , \blacklozenge). p_{O_2} in atm = 0.05 (open symbols), 0.10 (closed symbols).

and T_p for nine chars and petroleum coke. Original data on R_c and n have been used to calculate ρ_c at a common oxygen pressure of 1 atm, by Eq. (31). The Arrhenius parameters and other relevant data for the carbons in Fig. 8 are shown in Table I.

At 2000 K the highest reactivities are shown by chars from US coals (Pittsburgh and Illinois)¹⁰⁷ which are a factor of 10 higher than petroleum coke. At the same temperature the reactivities of a number of chars (from Millmerran sub-bituminous and Yalourn brown coals, Australia; anthracites and semi-anthracites, UK and western Europe; Ferrymoor and Brodsworth bituminous coals, UK) are about

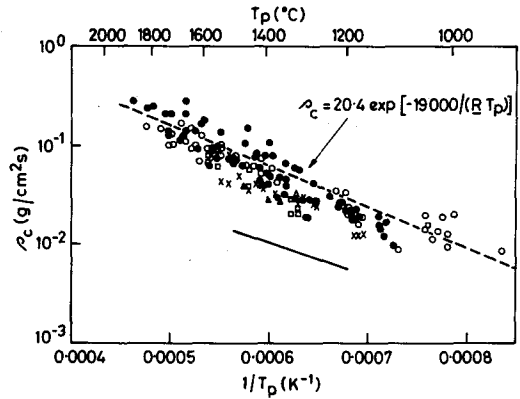


FIG. 7. Combustion rate data for anthracites and semi-anthracites (\bullet 78, 49, 22 μm ;⁹⁸ \circ 72, 42 μm ;⁹⁷ \times 28, 25 μm ;⁹⁵ \blacktriangle 31, 24, 23 μm ;⁹⁴ \triangle polydisperse single value;¹⁰³ \square polydisperse;¹⁰⁴ — polydisperse¹⁰⁵).

a factor of three higher than petroleum coke. However both the US materials, like the East Hetton char, show a steep decline in reactivity with temperature ($E \approx 34$ kcal/mol). At 1430 K the rate for the East Hetton char falls below that of petroleum coke, whilst at the same temperature (assuming extrapolation is justified) the US coals would show reactivities similar to the chars from the Australian coals, the anthracites and semi-anthracites, and so on.

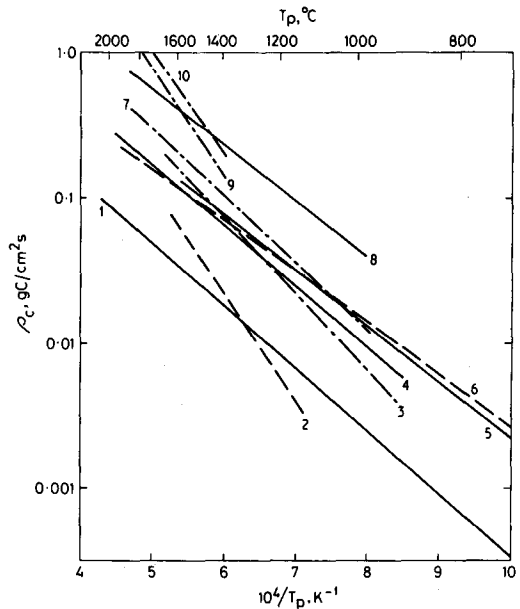


FIG. 8. Burning rates of coke and chars, $p_{\text{O}_2} = 1$ atm (see Table I for key).

TABLE I
 Data for coal chars in Fig. 8

Line no.	Parent coal	Pre-exponential factor (g/cm ² s (atm) ⁿ)	Activation energy (kcal/mol)	Appar-ent order of reaction	Particle size (μm)	Reference
1	Petroleum coke	7.0	19.7	0.5	18,77,85,88	49,98
2	East Hetton, swelling bituminous coal, UK	635.8	34.0	1.0	72	95
3	Brodsworth, swelling bituminous coal, UK	111.3	24.1	1.0	31	95
4	Anthracites and semi-anthracites, UK and western Europe	20.4	19.0	1.0	78,49,22,72,42	95,97
5	Millmerran, non-swelling, sub-bituminous coal, Australia	15.6	17.5	0.5	85	100
6	Yallourn brown coal, Australia	9.3	16.2	0.5	89,49	47
7	Ferrymoor, non-swelling bituminous coal, UK	70.3	21.5	1.0	34	95
8	Whitwick, non-swelling bituminous coal, UK	50.4	17.7	1.0	27	95
9	Pittsburgh seam, swelling bituminous coal, USA	4187.0	34.0	0.17	16	107
10	Illinois No. 6, swelling bituminous coal, USA	6337.0	34.1	0.17	13	107

In making the foregoing comparison the data were brought together on a common basis by extrapolating, in many cases by a factor of 10 or more, the effect of oxygen pressure above that used experimentally. However, the parameter used in making this extrapolation—the apparent reaction order—is often uncertain. Much of the information given in Fig. 8 applies to a single size of a given char. Coal is not a homogeneous material: different size fractions give rise to chars of different pore structures and chemical properties, thus giving rise to differing reactivities. Particle size also has an effect on the rate-control regime under which particles burn. All else being equal, fine particles can burn under regime I and coarse particles under regime II conditions. Thus the effects of temperature and oxygen concentration, and the mode of change of particle size and density with burn-off, all depend on particle size.

The data for the US coals show activation energies of about 34 kcal/mol and reaction orders of about 0.2. These facts, together with the small size of the particles (13 and 16 μm) suggest that combustion was under regime I conditions or in the transition between regimes I and II.

Intrinsic Chemical Reactivity Coefficient, R_i

The preceding discussion shows that the observed reactivity of coal chars, as manifest by the

rate coefficient, R_c , and the rate, ρ_c , differ for different types of coal. It is also shown that the value of R_c combines the separate effects of the intrinsic reactivity of the carbon and the extent and accessibility of the internal pore surface of the char. Specific surface areas vary from about 1 m²/g for petroleum coke to nearly 1000 m²/g for brown coal char.⁵⁹ So, to what extent do chemical or physical differences in various carbons affect the observed differences in reactivities? To answer this question it is necessary to know the coefficient of intrinsic chemical reactivity, R_i , defined by Eq. (14).

Smith⁵⁹ has used published data to calculate R_i for a wide range of porous carbons, including many chars, metallurgical coke, petroleum coke, pitch coke, nuclear graphite, carbon laid down on cracking catalyst and various highly-purified carbons. Reference 59 gives the data sources and essential information on the carbons concerned.

The results are shown in Fig. 9, where the intrinsic reaction rate, ρ_i , is at an oxygen pressure of 1 atm. ρ_i is calculated from:

$$\rho_i = R_i (p_{O_2})^m \quad \text{g/cm}^2\text{s} \quad (32)$$

an equation analogous to Eq. (31), and used for the same reason, namely to allow comparison of materials which show different values of reaction order m . ρ_i shows an activation energy of ~40 kcal/mol, the value previously noted to be expected for

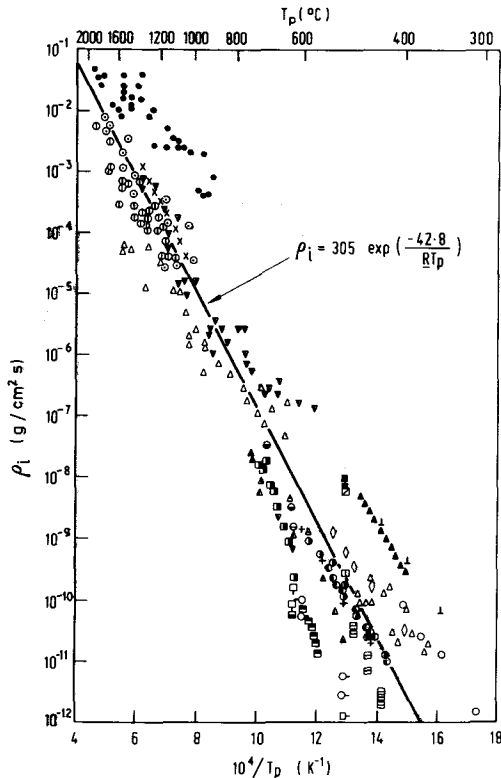


FIG. 9. Intrinsic reactivity of various carbons when $p_{O_2} = 1$ atm.

- } Petroleum coke
- ▲ } Petroleum coke
- } Petroleum coke
- △ } Brown-coal char
- } Lignite char
- ⊙ } Anthracite
- △ } Anthracite
- ⊕ } Semi-anthracite
- ▽ } Bituminous-coal char
- } Metallurgical coke
- × } Soot
- ⊠ } Pitch coke
- ◇ } Pitch resin
- ⊠ } Nuclear graphite
- △ } Nuclear graphite
- ⊕ } Nuclear graphite
- +
- ⊥ } Cracker carbon (uncatalysed)
- ⊥ } Cracker carbon (catalysed)
- ⊠ } AGKSP graphite
- ▲ } AGKSP graphite
- } AGKSP graphite
- } AUF
- ⊠ } SPI
- ⊠ } SPI
- ⊠ } SPI
- ⊠ } Spectroscopic graphite
- ▲ } Spectroscopic graphite

the reaction of impure carbons with oxygen. Figure 9 shows that there are large differences in reactivity between different carbons, even though effects due to different pore sizes and surface areas have been eliminated. For example at 775 K the intrinsic reactivity of petroleum coke is four orders of magnitude higher than that of graphon, and two orders of magnitude higher than that of nuclear graphite. At 1250 K the reactivity of petroleum coke is 1000 times higher than that of chars from brown coal and lignite. It is striking that petroleum coke shows the highest intrinsic reactivity (as distinct from the net reactivity per particle) of all but two of the carbons shown in Fig. 9.

The wide range of reactivities presumably reflects the effects of the atomic structure of the carbons, as well as the effects of impurities in the solid and gaseous reactants. Included in Fig. 9 are data from experiments with highly-purified carbons and oxygen, where differences in atomic structure of the carbons may be at a minimum. These data are shown separately in Fig. 10. The results from six separate series of experiments show similar intrinsic reactivities. The results of Lang *et al.*¹⁰⁸ are especially notable. They measured the intrinsic reactivity of 15 carbons, ranging from nuclear and spectroscopic graphites to sugar and wood charcoals. These materials, before further treatment, showed widely different intrinsic reactivities. However, after the carbon had been heat treated at 2973 K or above, and after several of the carbons had been exposed to chlorine at high temperatures, all the materials show similar reactivities. At 893 K the highest and lowest values of ρ_i (shown in Figs. 9 and 10) differed only by a factor of three. The preliminary heat treatment given to the carbons would have reduced the impurity levels substantially, but would also have caused a rearrangement of the carbon atoms to a more ordered structure. It is not yet clear which change would have the most effect.

The discussion of R_i and R_c show limited areas where common data exist: similar intrinsic reactivities are found for the purified carbons just mentioned, and observed reactivities (R_c) of similar magnitude are found for anthracites and semi-anthracites (Fig. 7). The wide variations found for R_c and R_i and the uncertainties in n and m show that there is still a strong need to gain a unifying understanding of carbon reactivity. More pragmatically there is a need to determine R_c for engi-

- } Graphon
- } Purified carbons
- } Sterling FT
- ▽ } Acheson NC
- ▽ } Acheson AFC 4

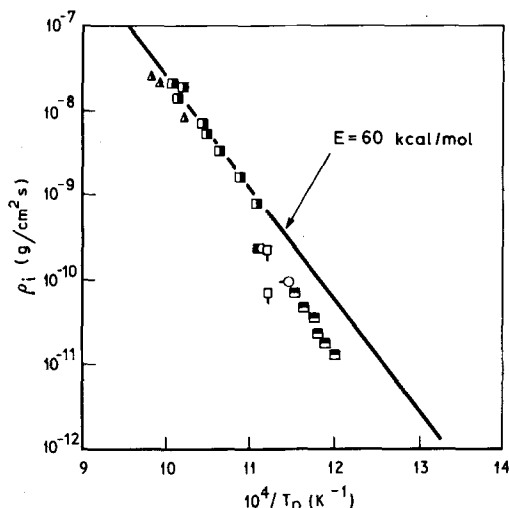


FIG. 10. Oxidation rate of highly purified carbons when $p_{O_2} = 1$ atm (see Fig. 9 for key).

neering purposes for each char considered at relevant temperatures and oxygen concentrations, and indeed for a range of particle sizes for a given char.

Mass Transfer Coefficient, h_m

The first data on the mass transfer coefficient, h_m , considered here are for pf-sized particles. It has been asserted that Eq. (24) is satisfactory for calculating mass transfer rates in pf flames. Figure 11 shows the calculated variation of ρ_m (the product $h_m C_g$) with temperature for 82 and 105 μm char particles burning at 0.1 atm of oxygen for car-

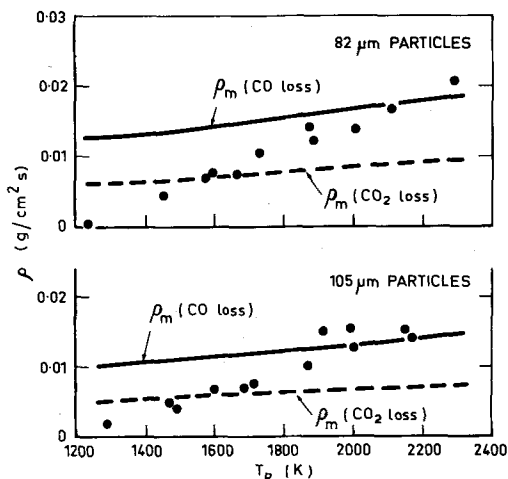


FIG. 11. Comparison of measured and theoretical maximum burning rates when $p_{O_2} = 1$ atm.⁹¹

bon loss as CO and CO₂. The data points (values of ρ reported by Field⁹¹) rise to, and lie closely about, the CO-loss line. The fact that some of the measured values of ρ lie slightly above the calculated "maximum possible" value of ρ_m arises from experimental error and because ρ_m was calculated for the initial particle size, a dimension that decreases as particles burn, with corresponding higher values for ρ_m . Equation (24) shows h_m , and hence ρ_m , vary inversely with particle size.

A number of other kinetics experiments with various pf chars^{47,49,91,98} show values of ρ that rise to, but do not significantly exceed, the corresponding values of ρ_m calculated for carbon loss as CO. Larger-scale experiments in which polydisperse pf suspensions have been burned at high intensities also support the validity of calculating h_m by Eq. (24). Hoy *et al.*¹⁰⁹ operated an MHD combustor at ~ 2600 K and up to 6 atm pressure. The measured combustion efficiencies and heat release rates agreed well with those calculated assuming the variously-sized particles burned away with $\rho = \rho_m$ and carbon removed from the particles as CO. More recently Farzan and Essenhigh¹¹⁰ burned pf at atmospheric pressure but at temperatures above 2000 K. The measured combustion behaviour agreed with that calculated with ρ set equal to ρ_m .

There is ample evidence that for particles larger than pf, i.e. >0.1 in size, in isolation or in packed beds, the mass transfer rates can be calculated with confidence by Eq. (23).^{36,82,83} For example the burning times of larger particles, calculated setting $\rho = \rho_m$, agree well with experiment.¹¹ Roberts and Smith¹¹¹ showed that the measured burning rates for 6 mm spheres of graphite immersed in flowing streams of cold, dry, oxygen agreed with the calculated mass transfer rates.

Roberts and Smith¹¹¹ also showed that the measured temperatures of the burning spheres were close to those calculated assuming carbon loss as CO. Likewise Ayling and Smith¹¹² found agreement between measured and calculated values of T_p for pulverized semi-anthracite particles, for carbon loss as CO. Recently workers at Sandia¹¹³ reported good agreement between measured and calculated values of T_p , assuming carbon loss as CO, for petroleum coke and Millmerran coal char. It has been noted that CO is the primary product of the oxygen-carbon reaction at flame temperatures, but the location of the subsequent CO-oxidation zone can affect both h_m and T_p . Early estimates^{3e} of the location of this zone show it to be sufficiently far away from pf-sized particles not to have a notable effect on their burning. However for particles >1 mm CO-oxidation was estimated to take place on the particle surface, with the carbon loss effectively as CO₂. Recent, and more complex, calculations by Amundson and co-workers^{114,115} support this conclusion.

The matters dealt with so far in this section are concerned with small particles in entrainment and larger particles (singly or in beds) fixed in relation to a known flow of gas. It has already been noted that the situation in fluidized-bed combustion is more complex and less well understood. Considering only the step of oxygen transport through the dense, inert phase of the fluidized bed to the burning particle (see Fig. 2 and the relevant discussion) the problem is to determine the appropriate coefficient for mass transfer. Mass transfer in the dense phase of fluidized beds is not yet well understood, and indeed there are conflicting interpretations of the relevant data.^{83,85,86} However, for the situation in fluidized-bed combustion, where the active particles are dispersed and well-diluted in a bed of inert particles, relationships of the form of Eq. (23), modified along the lines used in Eq. (25), can be used with some success. Avedesian and Davidson⁴⁵ argued that in the dense phase of fluidized beds, where the gas velocity is low, the Sherwood number (Sh) is close to 2. However more recent studies^{34,84,116} show values of Sh of 4 or more under fluidized-bed combustion conditions.

For these circumstances there are difficulties in gaining adequate knowledge of Sh . Satisfactory determinations require a measurement of the particle's burning rate, means of accounting for the extent that chemical rate control affects this rate, a knowledge of particle temperature and an understanding of whether the O_2 diffusing to the particle leaves it as CO or CO_2 . Recently La Nauze and Jung⁸⁴ made careful measurements of the burning rates of single petroleum coke spheres (in air) immersed in a fluidized sand bed (so avoiding rate restrictions due to bubble-to-bed transfer). The appropriate values of R_c and n were already known from the measurements on the same material.⁴⁹ Hence ρ_m and Sh could be calculated, given that the value of T_p was known and the manner of loss of carbon as CO or as CO_2 . Reliable calculations of T_p by Eq. (2) are not possible; the knowledge of heat transfer between burning particles and fluidized beds is at least as uncertain as the mass transfer process. La Nauze and Jung,⁸⁴ on the basis of visual estimates of particle temperature, give weight to carbon leaving the particle as CO_2 , calculating R_c , h_m , and Sh on this basis. More recently these workers have measured particle temperatures using embedded thermocouples; the measured temperatures are close to those calculated for CO_2 loss. Figure 12 compares the measured relation between Sh and particle size with the value calculated by Eq. (25) for carbon loss as CO_2 . The agreement between theory and experiment is good. Nonetheless more insight is needed into mass (and heat) transfer in fluidized-bed combustion and into suitable means of determining T_p .

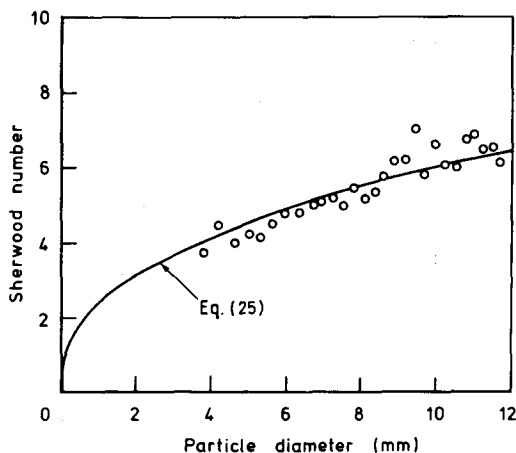


FIG. 12. Measured and calculated values of the Sherwood number in a fluidized-bed combustor (from La Nauze and Jung).⁸⁴

Changes in Particle Structure During Combustion

It has already been pointed out that the size, density, porosity, pore size, and pore surface area have important effects on the combustion behaviour of particles. In summary, where combustion is limited to the outer surface of the particle or to a shallow zone below the outer surface, particles will burn with constant density but with a steady reduction in size. When oxygen penetrates completely within a particle's pore structure, combustion occurs at constant size but with decreasing density. For pf-sized particles burning in regime II conditions the penetration depth of oxygen is of the order of particle radius, consequently these particles burn with reduction in both size and density. Thin-walled cenospheres burn with reducing density but at constant size whether oxygen penetrates the pores or not.

In regime II conditions, as pore diffusion plays a major role, it is important to have data on the opening of pores and changes in pore surface. In regime I it is important to understand the development of pore surface area during combustion.

Changes in Particle Size and Density

Figure 13 shows the change in size and density with burn-off for a sphere of petroleum coke burned in a fluidized bed. The burning rate was controlled mainly by oxygen diffusion to the particle.⁸⁴ The change in size with burn-off decreases steadily in the manner shown by Eq. (29) with $\alpha = 1/3$, whilst there is little change in particle density, as

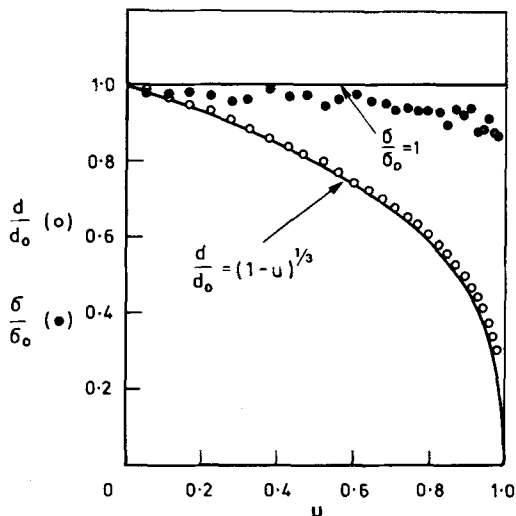


FIG. 13. Changes in particle size and density with burn-off in a fluidized-bed combustor (from La Nauze and Jung).⁸⁴

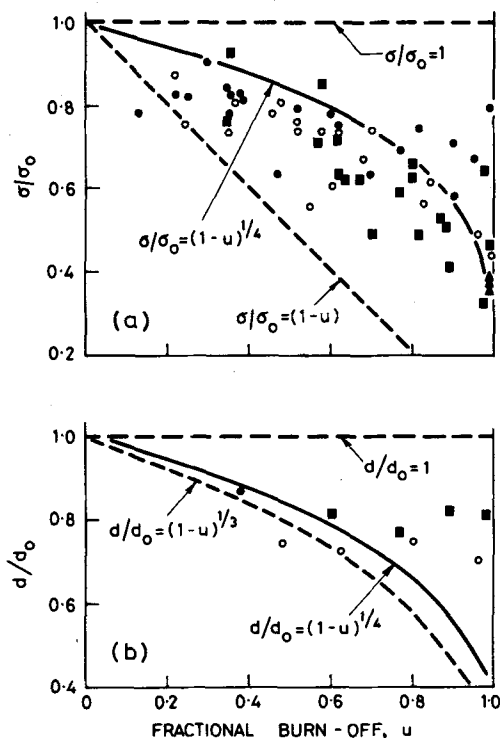


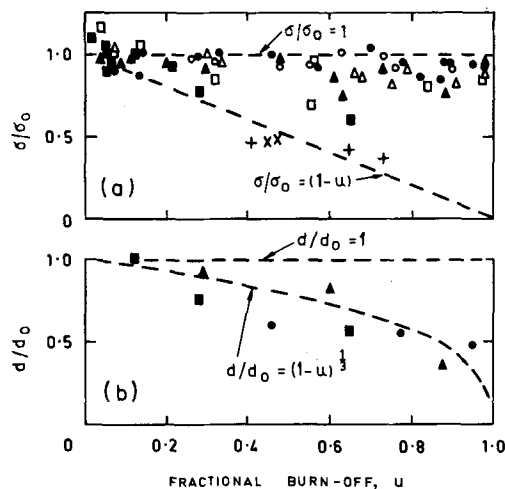
FIG. 14. Relation between burn-off and (a) particle density and (b) particle size, for semi-anthracite (particle size: ● 78 μm , ○ 49 μm , ■ 22 μm , ▲ 6 μm).

should be the case when external mass-transfer in the main limitation of the rate.

Figure 14 shows changes in size and density with burn-off for size graded particles of pulverized semi-anthracite.⁹⁷ The data, though scattered, show steady reductions in both size and density and can be represented by Eqs. (29) and (30), with $\alpha = \beta = 1/4$. This is the expected result for regime II conditions which, from other measurements, were shown to apply during the experiments considered.⁹⁷

The data in Fig. 15 show the changes in size and density with burn-off for 89, 49, and 22 μm particles of brown coal char.⁴⁷ With the exception of the 22 μm fraction there is little change in density ($\beta = 0$ in Eq. (30)), but the size reduces steadily ($\alpha = 1/3$ in Eq. (29)). In fact diffusion of oxygen to the particles had a major rate-controlling effect for the 89 and 49 μm particles⁴⁷, and the observed changes in size and density are consistent with this fact. However, the density of the 22 μm fraction reduced steadily with burn-off ($\beta = 1$ in Eq. (30)) in a manner consistent with regime I conditions, which in fact were shown to apply for these particles.^{47,48}

Data are also available on the variation of size and density during the combustion of chars from



p_{O_2} atm:	ENTRAINMENT REACTOR		FIXED-BED REACTOR
	0.2	0.1	0.1
$d_0, \mu\text{m}$ {	89 ●	○	+
	49 ▲	△	x
	22 ■	□	

FIG. 15. Relation between burn-off and (a) particle density and (b) particle size, for a brown coal char.

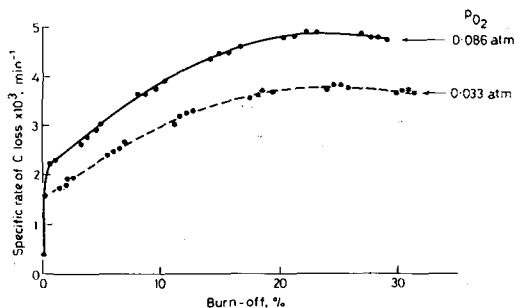


FIG. 16. Variation of observed reaction rate with burn-off.¹¹⁷

a swelling bituminous coal from New Zealand⁸⁹ and a number of British bituminous coals.⁹⁵

Changes in Pore Surface Area

The effects of changes in pore surface area can be significant for combustion in regimes II and I, but especially so in the latter as the rate is directly proportional to the surface area of the pores (Eq. (16)). The well-known fact that rates can change with burn-off under regime I conditions is illustrated in Fig. 16, adapted from the study of graphite oxidation by Tyler *et al.*¹¹⁷ The specific rate of oxidation (per unit weight of carbon burning) increased until about 25% burn-off, and then started to decline. That specific surface areas can pass through a maximum during combustion is shown in Fig. 17, using data on the oxidation of anthracite.¹¹⁸ The direct relation between reactivity and

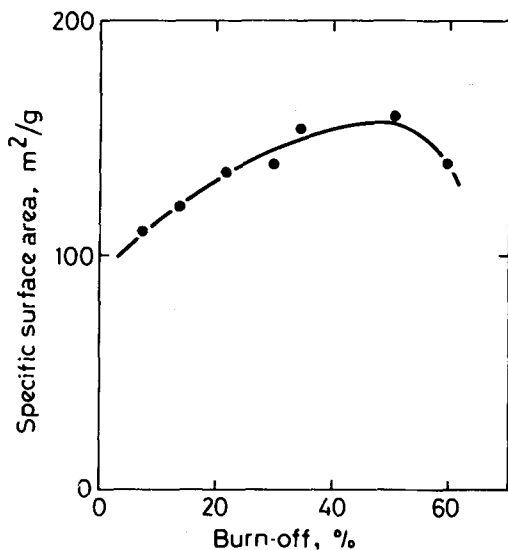


FIG. 17. Variation of specific surface area with burn-off.¹¹⁸

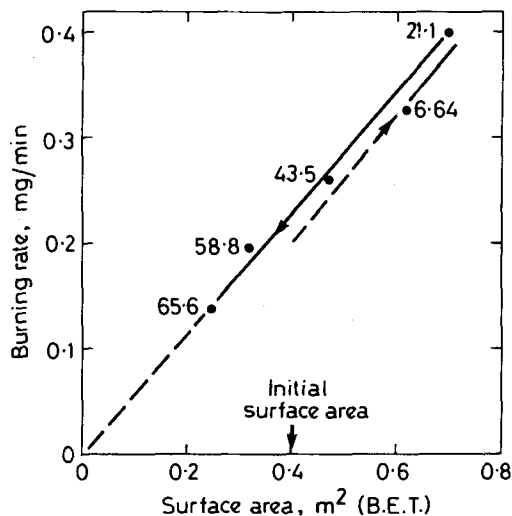


FIG. 18. Relationship between burning rate and pore surface area¹¹⁹ (numbers denote % burn-off).

pore surface area is shown in Fig. 18, for the oxidation of spectroscopic graphite.¹¹⁹ The numbers on the line denote percent burn-off and the data show the linear variation of rate with the development of surface area during reaction.

Some data have been published on the development of pore surface area during the combustion of pf chars.^{48,58} In the case of semi-anthracite particles⁵⁸ areas reduced steeply with increasing burn-off. It was shown, however, that the reduction could well be due to annealing away of the fine pores, as the data at high levels of burn-off were produced at high combustion temperatures (~ 2000 K).

In the earlier section on pore diffusion coefficients a number of references are given to models of the development of pore structures during the combustion and gasification of carbon. Most of the papers contain experimental data on pore structures or related matters which are compared with the corresponding theoretical predictions.

Concluding Remarks

It has been shown that there are relationships by which the burning rates of coal chars and particle temperatures can be calculated, accounting for mass transfer of oxygen to the particles, diffusion into the pore structure and chemical reaction on the pore walls.

There are many data on the rate coefficient, R_c , for pf chars and similar materials. However R_c , which combines the effects of pore diffusion and intrinsic chemical reactivity, varies notably in ab-

solute value and in temperature dependence from char to char, only showing similar values for similar types of material, i.e. anthracites and semi-anthracites. Furthermore, R_c can vary with particle size for a given char. The effect of oxygen pressure on R_c , i.e. the observed reaction order n , is uncertain.

Given adequate information on the pore structure of carbons it is possible to separate the chemical and physical contributions to the value of R_c . The intrinsic chemical reactivity coefficient, R_i (or rate, ρ_i) so determined varies widely with the type of carbon. At a given temperature for different carbons, differences of reactivity of up to four orders of magnitude are found.

It is possible to calculate R_c (and hence the reaction rate, ρ) from a knowledge of R_i and data on the pore structure, assuming the latter is in a steady state. Mathematical models are now being developed that allow, in principle, the calculation of the way pore structure develops during combustion from some initial value. However, the models do not yet fully account for the complex nature of the pore structure of coal chars.

In general, then, there is as yet no unifying approach to understanding the reactivity of impure carbons (i.e. coal chars) to oxygen. Where required for engineering purposes it is necessary to determine R_c for chars made from coals under conditions appropriate to the type of combustion system of interest. The response of R_c to temperature, oxygen concentration and particle size needs to be known for each type of char.

To gain a deeper insight into the combustion process it is necessary to have better experimental information on the pore structure of particles, especially on the pore diffusion coefficient, coupled with improved models of developing pore systems. Related experiments are needed to understand why R_i varies so widely for different carbons. The roles of impurities and the atomic structures of carbons need further investigation.

The mass transfer of oxygen to particles is well understood for pf systems and for large burning particles in gases of well-defined flow properties. The situation for fluidized-bed combustion is much less well understood, as are the related matters of particle temperature and whether carbon is lost from the particle as CO or CO₂.

To satisfy the needs outlined above, experiments are required that include the following; the use of modern optical techniques to give information on particle temperature and velocity, together with detailed descriptions of the behaviour of pf chars burning in laboratory flames, coupled with accurate measurements of combustion rates in the same flames; the development of techniques to determine the pore structure properties of chars (especially the pore diffusion coefficient) at temperatures approaching those found in flames; the determi-

nation of R_i where pore diffusion effects are absent (e.g. for very fine particles at flame temperatures); the measurement of mass transfer rates to fuel particles burning in fluidized beds, coupled with temperature measurements on the burning particles.

In addition to those matters directly related to char combustion there is a need to have much more information on the devolatilization process of coal, particularly on the devolatilization kinetics of materials at sizes appropriate to pf and fluidized-bed combustion. The kinetic experiments should involve atmospheres and heating environments appropriate to the combustors considered. Data are also required on the chemical and physical properties of the chars produced during devolatilization.

Nomenclature

A	pre-exponential factor	$\text{g/cm}^2\text{s(atm)}^n$
A_g	specific pore-surface area	cm^2/g
A_o	fractional consumption of oxygen	
B	constant	
C_g	oxygen concentration in bulk gas	g/cm^3
C'_g	oxygen concentration in dense phase	g/cm^3
C_p	specific heat of particle	cal/g mol K
C_s	oxygen concentration on particle's outer surface	g/cm^3
D	bulk gas diffusion coefficient	cm^2/s
D_e	effective diffusion coefficient in porous solid	cm^2/s
D_p	pore diffusion coefficient	cm^2/s
d	particle size	cm
d_b	bubble diameter	cm
E	activation energy	kcal/mol
g	gravitational acceleration	cm/s^2
H	heat of reaction	cal/g
h_m	mass transfer coefficient—carbon oxide flux	cm/s
h'_m	mass transfer coefficient—oxygen flux	cm/s
h_o	initial height of fluidized bed	cm
k'	function of particle combustion rate (Eq. (7))	
M	molecular weight	g/g mol
m	true order of reaction	
n	apparent order of reaction	
o	(subscript) denotes initial or reference conditions	
P	combustor pressure	atm, kPa
P_o	reference pressure	atm, kPa

p_{O_2}	partial pressure of oxygen	atm, kPa
R	gas constant	$\text{cm}^3 \text{ atm/g mol K}$
R_c	rate coefficient per unit external surface area	$\text{g/cm}^2 \text{ s (atm)}^n$
R_i	intrinsic rate coefficient	$\text{g/cm}^2 \text{ s (atm)}^m$
Re	Reynold's number	
\bar{r}_p	mean pore radius	cm
Sc	Schmidt number	
Sh	Sherwood number	
T_g	gas temperature	K
T_m	mean temperature in boundary layer	K
T_p	particle temperature	K
T_s	radiation temperature	K
t	time	s
U_b	bubble velocity	cm/s
U_m	minimum fluidizing velocity	cm/s
u	fractional burn-off	
V_c	volume fraction of carbon in fluidized bed	
W	weight of particle	g
X	number of times a bubble is flushed out (Eq. (5))	
x	ratio of initial outside to inside diameter of hollow particle	
y	$1 - u$	
Z	U_b/U_m	
α	coefficient for particle size change (Eq. (27))	
β	coefficient for particle density change (Eq. (28))	
γ	characteristic size of particle	cm
γ_o	function of Z (Eq. (4))	
ϵ	voidage	
η	effectiveness factor	
θ	porosity of particle	
κ	reaction order (Eq. (19))	
ρ	actual (observed) rate of combustion of carbon per unit external surface area of the particle	$\text{g/cm}^2 \text{ s}$
ρ_c	reaction rate	$\text{g/cm}^2 \text{ s}$
ρ_i	intrinsic reaction rate (Eq. (32))	$\text{g/cm}^2 \text{ s}$
ρ_m	maximum reaction rate	$\text{g/cm}^2 \text{ s}$
σ	particle density	g/cm^3
τ	tortuosity of pores	
ϕ	Thiele modulus	
ϕ_1	term involving conductive heat transfer (Eq. (2))	cal/g s K

ϕ_2	term involving radiative heat transfer (Eq. (2))	cal/g s K^4
χ	ratio ρ/ρ_m	

Acknowledgments

The author is indebted to many people for their contributions to this review. Particular thanks are due to R. H. Essenhigh and J. B. Howard for providing the opportunity to give this review, and to R. H. Essenhigh for his guidance in its preparation. W. J. McLean and W. R. Seeker kindly supplied the photographs for Fig. 1. Unpublished data have been provided by R. H. Essenhigh, H. Farzan, K. Jung, G. Kothandaraman, R. D. LaNauze, W. J. McLean, R. E. Mitchell and G. A. Simons.

REFERENCES

- ESSENHIGH, R. H.: *J. Inst. Fuel* 34, 16 (1961).
- MULCAHY, M. F. R.: *Oxygen in Metal and Gaseous Fuel Industries*, p. 175, The Chemical Society, London, 1978.
- FIELD, M. A., GILL, D. W., MORGAN, B. B. AND HAWKSLEY, P. G. W.: *Combustion of Pulverized Coal*, The British Coal Utilization Research Association, Leatherhead, 1967 (a) p. 216, (b) p. 301, (c) p. 189, (d) p. 305, (e) p. 201.
- SMOOT, L. D. AND PRATT, D. T. (Eds): *Pulverized-coal Combustion and Gasification*, Plenum Press, New York, 1979.
- THRING, M. W. AND ESSENHIGH, R. H.: *Chemistry of Coal Utilization* (H. H. Lowry, Ed.), Suppl. Vol., Ch. 17, John Wiley, New York, 1963.
- ESSENHIGH, R. J., FROBERG, R. AND HOWARD, J. B.: *Ind. Eng. Chem.* 57, 32 (1965).
- GRAY, D., COGOLI, J. G. AND ESSENHIGH, R. H.: in *Coal Gasification* (L. G. Mossey, Ed.), p. 72, *Advances in Chemistry Series 131*, American Chemical Society, 1974.
- ESSENHIGH, R. H.: *Sixteenth Symposium (International) on Combustion*, p. 353, The Combustion Institute, Pittsburgh, 1977.
- ESSENHIGH, R. H.: *Chemistry of Coal Utilization* (M. A. Elliot, Ed.), 2nd Suppl. Vol., Ch. 19, John Wiley, New York, 1981.
- WENDT, J. O. L.: *Prog. Energy Combust. Sci.* 6, 201 (1980).
- MULCAHY, M. F. R. AND SMITH, I. W.: *Rev. Pure Appl. Chem.* 19, 81 (1969).
- HEDLEY, A. B. AND LEESLEY, M. E.: *J. Inst. Fuel* 38, 492 (1965).
- LAURENDEAU, N. M.: *Prog. Energy Combust. Sci.* 4, 221 (1978).
- SMITH, I. W.: *Conference on Coal Combustion*

- Technology and Emission Control*, California Institute of Technology, Pasadena, 1979, unpublished.
15. SMITH, I. W.: in *Pulverized Coal Combustion: Pollutant Formation and Control* (A. F. Sarofim, Ed.), EPA Monograph, in press.
 16. JÜNGTEN, H. AND VAN HEEK, K. H.: *Fuel Process. Technol.* 2, 261 (1979).
 17. ANTHONY, D. B. AND HOWARD, J. B.: *AIChE J.* 22, 625 (1976).
 18. HOWARD, J. B.: Coal pyrolysis—product yields and products: survey, *EPRI Conference on Coal Pyrolysis*, Palo Alto, 1981.
 19. HOWARD, J. B.: *Chemistry of Coal Utilization* (M. A. Elliot, Ed.), 2nd Suppl. Vol., Ch. 12, John Wiley, New York, 1981.
 20. SMITH, I. W.: New approaches to coal pyrolysis—CSIRO, *EPRI Conference on Coal Pyrolysis*, Palo Alto, 1981.
 21. SEEKER, W. R., SAMUELSEN, G. S., HEAP, M. P. AND TROLLINGER, J. D.: *Eighteenth Symposium (International) on Combustion*, p. 1213, The Combustion Institute, Pittsburgh, 1981.
 22. MCLEAN, W. J., HARDESTY, D. R. AND POHL, J. H.: *Eighteenth Symposium (International) on Combustion*, p. 1239, The Combustion Institute, Pittsburgh, 1981.
 23. THOMAS, G. R., HARRIS, I. R. AND EVANS, D. G.: *Combust. Flame* 12, 391(1968).
 24. LESLIE, I., JOST, M. AND KRUGER, C.: *Oxidation Reactivity of Pulverized Montana Rosebud Coal During Combustion*, Spring Meeting, Western States Section, The Combustion Institute, Los Angeles, 1982.
 25. JÜNGTEN, H. AND VAN HEEK, K. H.: *Fuel* 47, 103 (1968).
 26. KIMBER, G. M. AND GRAY, M. D.: *Combust. Flame* 11, 360 (1967).
 27. STREET, P. J., WEIGHT, R. P. AND LIGHTMAN, P.: *Fuel* 48, 343 (1969).
 28. TYLER, R. J.: *Fuel* 58, 680 (1979).
 29. TYLER, R. J.: *Fuel* 59, 218 (1980).
 30. BADZIOCH, S. AND HAWKSLEY, P. G. W.: *Ind. Eng. Chem., Proc. Des. Dev.* 9, 521 (1970).
 31. NSAKALA, N. YA, ESSENHIGH, R. H. AND WALKER, P. L.: *Combust. Sci. Technol.* 16, 153 (1977).
 32. KOBAYASHI, H., HOWARD, J. B. AND SAROFIM, A. F.: *Sixteenth Symposium (International) on Combustion*, p. 411, The Combustion Institute, Pittsburgh, 1977.
 33. SCARONI, A. W., WALKER, P. L. AND ESSENHIGH, R. H.: *Fuel* 60, 71 (1981).
 34. PILLAI, K. K.: *J. Inst. Energy* 54, 143 (1981).
 35. LA NAUZE, R. D.: in *Fluidization* (J. F. Davidson, D. Harrison and R. Clift, Eds), Ch. 19, Academic Press, London, in prep.
 36. BEÉR, J. M.: *Sixteenth Symposium (International) on Combustion*, p. 439, The Combustion Institute, Pittsburgh, 1977.
 37. GIBSON, M. M. AND MORGAN, B. B.: *J. Inst. Fuel* 43, 517 (1970).
 38. XIEU, D. V., MASUDA, T., GOGOLI, J. G. AND ESSENHIGH, R. H.: *Eighteenth Symposium (International) on Combustion*, p. 1461, The Combustion Institute, Pittsburgh, 1981.
 39. LOWE, A., WALL, T. F. AND STEWART, I. MCC.: *Fifteenth Symposium (International) on Combustion*, p. 1261, The Combustion Institute, Pittsburgh, 1975.
 40. MCKENZIE, A. AND SMITH, I. W.: *Numerical Simulation of Pulverized-fuel Combustion*, CSIRO Division of Mineral Chemistry, Investigation Report 91, 1973.
 41. MCKENZIE, A., SMITH, I. W. AND SZPINDLER, G. A. D.: *J. Inst. Fuel* 47, 75 (1974).
 42. GORDON, A. L. AND AMUNDSON, N. R.: *Chem. Eng. Sci.* 31, 1163 (1976).
 43. GORDON, A. L., CARAM, H. S. AND AMUNDSON, N. R.: *Chem. Eng. Sci.* 33, 713 (1978).
 44. WELLS, J. W., CULVER, M. H. AND KRISHNAN, R. P.: *Tennessee Valley Authority Atmospheric Fluidized-bed Combustor Simulation Interim Annual Report*, ORNL/TM-7847, Oak Ridge National Laboratory, 1981.
 45. AVEDESIAN, M. M. AND DAVIDSON, J. F.: *Trans. Inst. Chem. Eng.* 51, 121 (1973).
 46. LEUNG, L. S. AND SMITH, I. W.: *Fuel* 58, 354 (1979).
 47. HAMOR, R. J., SMITH, I. W. AND TYLER, R. J.: *Combust. Flame* 21, 153 (1973).
 48. SMITH, I. W. AND TYLER, R. J.: *Combust. Sci. Technol.* 9, 87 (1974).
 49. YOUNG, B. C. AND SMITH, I. W.: *Eighteenth Symposium (International) on Combustion*, p. 1249, The Combustion Institute, Pittsburgh, 1981.
 50. ARIS, R.: *Chem. Eng. Sci.* 6, 262 (1957).
 51. THIELE, E. W.: *Ind. Eng. Chem.* 31, 916 (1939).
 52. MEHTA, B. N. AND ARIS, R.: *Chem. Eng. Sci.* 26, 1699 (1971).
 53. WALKER, P. L., RUSINKO, F. AND AUSTIN, L. G.: *Adv. Catal.* 11, 133, (1959).
 54. ROSSBERG, M. AND WICKE, E.: *Chem. -Ing. -Tech.* 29, 181 (1956).
 55. FRANK-KAMENETSKII, D. A.: *Diffusion and Heat Transfer in Chemical Kinetics*, p. 103, Plenum Press, New York, 1969.
 56. SATTERFIELD, C. N.: *Mass Transfer in Heterogeneous Catalysis*, p. 56, Massachusetts Institute of Technology Press, 1970.
 57. WHEELER, A.: *Adv. Catal.* 3, 249 (1951).
 58. SMITH, I. W. AND TYLER, R. J.: *Fuel* 51, 312 (1972).
 59. SMITH, I. W.: *Fuel* 57, 409 (1978).

60. MINGLE, J. O. AND SMITH, J. M.: *AICHe J.* 7, 243 (1961).
61. CARBERRY, J. J.: *AICHe J.* 8, 557 (1962).
62. ÖRS, N. AND DOĞU, T.: *AICHe J.* 25, 723 (1979).
63. HASHIMOTO, K. AND SILVESTON, P. L.: *AICHe J.* 19, 259 (1973).
64. GRILLET, Y., REBAUDIERES, P. AND GUÉRIN, H.: *Bull. Soc. Chim. France* 7, 2423 (1967).
65. SIMONS, G. A.: *Combust. Sci. Technol.* 19, 227 (1979).
66. SIMONS, G. A. AND FINSON, M. L.: *Combust. Sci. Technol.* 19, 217 (1979).
67. SIMONS, G. A.: *Fuel* 59, 143 (1980).
68. SIMONS, G. A. AND KOTHANDARAMAN, G.: *Effects of Preignition in Pulverized Coal Combustion*, PSI 290, Physical Sciences Inc., 1981.
69. CHORNET, E., BALDASANO, J. M. AND TARKI, H. T.: *Fuel* 58, 395 (1979).
70. BHATIA, S. K. AND PERLMUTTER, D. D.: *AICHe J.* 26, 379 (1980).
71. SRIVINAS, B. AND AMUNDSON, N. R.: *AICHe J.* 26, 487 (1980).
72. GAVALAS, G. R.: *AICHe J.* 26, 577 (1980).
73. GAVALAS, G. R.: *Combust. Sci. Technol.* 24, 197 (1981).
74. SIMONS, G. A.: *Combust. Sci. Technol.* 24, 211 (1981).
75. GAVALAS, G. R.: *Combust. Sci. Technol.* 26, 212 (1981).
76. PETERSEN, E. E.: *AICHe J.* 3, 443 (1957).
77. HOSHIMOTO, K. AND SILVERSTON, P. L.: *AICHe J.* 19, 268 (1973).
78. RAMACHANDRAN, P. A. AND SMITH, J. M.: *AICHe J.* 23, 353 (1977).
79. KREIGBAUM, R. A. AND LAURENDEAU, N. M.: *Pore Model for the Gasification of a Single Coal Particle*, Proceedings of the Eastern States Section, The Combustion Institute, Hartford, 1977.
80. HOLVE, D. J.: *Extensions to the Analytical Model for Porous Char Particle Burnout*, Western States Section, The Combustion Institute, Los Angeles, 1980.
81. SRINIVAS, B. AND AMUNDSON, N. R.: *Can. J. Chem. Eng.* 59, 728 (1981).
82. KUNII, D. AND LEVENSPIEL, O.: *Fluidization Engineering*, p. 199, John Wiley, New York, 1969.
83. JOOS, F. M. AND GLICKSMAN, L. R.: *The Proper Values of the Sherwood and Nusselt Numbers for Individual Particles in Fired and Fluidized Beds*, Department of Mechanical Engineering, Massachusetts Institute of Technology, private communication, 1976.
84. LA NAUZE, R. D. AND JUNG, K.: *Nineteenth Symposium (International) on Combustion*, this vol., The Combustion Institute, Pittsburgh, 1982.
85. NELSON, P. A. AND GALLOWAY, T. R.: *Chem. Eng. Sci.* 30, 1 (1975).
86. ROWE, P. N.: *Chem. Eng. Sci.* 30, 7 (1975).
87. GUNN, D. J.: *Int. J. Heat Mass Trans.* 21, 467 (1978).
88. SCHLÜNDER, E. U.: *Chem. Eng. Sci.* 32, 845 (1977).
89. SERGEANT, G. D. AND SMITH, I. W.: *Fuel* 52, 52 (1973).
90. RAMSDEN, A. R. AND SMITH, I. W.: *Fuel*, 47, 253 (1968).
91. FIELD, M. A.: *Combust. Flame*, 13, 237 (1969).
92. LITTLEJOHN, R. E.: *J. Inst. Fuel* 40, 128 (1967).
93. HEIN, K. AND SMITH, I. W.: *J. Inst. Fuel* 47, 162 (1976).
94. FIELD, M. A. AND ROBERTS, R. A.: *British Coal Utilization Research Association Memb. Inf. Circ.* 325 (1967).
95. FIELD, M. A.: *Combust. Flame* 14, 237 (1970).
96. MULCAHY, M. F. R. AND SMITH, I. W.: *Chemeca 70*, Session 2, p. 101, Butterworths, Australia, 1971.
97. SMITH, I. W.: *Combust. Flame* 17, 421 (1971).
98. SMITH, I. W.: *Combust. Flame* 17, 303 (1971).
99. YOUNG, B. C.: *International Conference on Coal Science*, p. 260, Verlag Glückauf, Essen, 1981.
100. YOUNG, B. C.: *The Burning of Char Particles in Entrainment*, Chemical Reaction Engineering Workshop, Monash University, 1979.
101. EDWARDS, J. H., SMITH, I. W. AND TYLER, R. J.: *Fuel* 59, 681 (1980).
102. PARK, C. AND APPLETON, J. P.: *Combust. Flame* 20, 369 (1973).
103. MARSDEN, C.: *Anthracite Dust Cloud Combustion*, Ph. D. thesis, University of Sheffield, 1964.
104. HEIN, K.: *Preliminary Results of C.15 Trials*, International Flame Research Foundation, P.F. Panel Meetings, August and December, 1970.
105. BEER, J. M., LEE, K. B., MARSDEN, C. AND THRING, M. W.: *Conference on Combustion and Energy Conversion*, paper 1.9, Institute Française des Combustibles et de l'Energie, 1964.
106. SMITH, I. W.: *Australian Research on Flash Pyrolysis*, AICHe Winter Meeting, Orlando, 1982.
107. LESTER, T. W., SEEKER, W. R. AND MERKLIN, J. F.: *Eighteenth Symposium (International) on Combustion*, p. 1257, The Combustion Institute, Pittsburgh, 1981.
108. LANG, F. M., MAGNIER, P. AND MAY, S.: *Fifth Carbon Conference*, Vol. 1, p. 171, Pergamon Press, New York, 1962.
109. HOY, H. R., ROBERTS, A. G. AND WILKINS, D. M.: *Coal Combustion in Open-cycle MHD Power Generators* (J. B. Heywood and G. J. Womak, Eds), p. 261, Pergamon Press, Oxford, 1969.
110. FARZAN, H. AND ESSENHIGH, R. H.: *Nineteenth*

- Symposium (International) on Combustion*, this vol., The Combustion Institute, Pittsburgh, 1982.
111. ROBERTS, O. C. AND SMITH, I. W.: *Combust. Flame* 21, 123 (1973).
 112. AYLING, A. B. AND SMITH, I. W.: *Combust. Flame* 18, 173 (1972).
 113. MITCHELL, R. E. AND MCLEAN, W. J.: *On the Temperature and Reaction Rate of Burning Pulverized Fuels*, Sandia National Laboratories, Livermore, private communication, 1982.
 114. CARAM, H. S. AND AMUNDSON, N. R.: *Ind. Eng. Chem. Fund.* 16, 171 (1977).
 115. MON, E. AND AMUNDSON, N. R.: *Ind Eng. Chem. Fund.* 17, 313 (1978).
 116. STANMORE, B. R. AND JUNG, K.: *Trans. Inst. Chem. Eng.* 58, 66 (1980).
 117. TYLER, R. J., WOUTERLOUD, H. J. AND MULCAHY, M. F. R.: *Carbon* 14, 271 (1976).
 118. JOZEFCAK-IHLER, M. AND GUÉRIN, H.: *Bull. Soc. Chim. France*, 2018 (1966).
 119. BONNETAIN, L. AND HOYNANT, G.: *Les Carbones*, Vol. 2, p. 277, Group Français d'Etude des Carbones, Masson et Cie, Paris, 1965.
 120. JAMALUDDIN, A. S., TRUELOVE, J. S. AND WALL, T. F. Private communication, University of Newcastle, NSW, 1982.